

Design and characterization of reversible thermodynamic SMPU-based fabrics with improved comfort properties

Volume 53: 1–20

© The Author(s) 2023

Article reuse guidelines:

sagepub.com/journals-permissions

DOI: 10.1177/15280837231166390

journals.sagepub.com/home/jit

Judit Gonzalez Bertran^{1,2,3} , Mònica Ardanuy²,
Marta González³, Rosa Rodriguez¹ and Petar Jovančić^{1,4}

Abstract

In recent years, great efforts have been made to research and develop advanced thermodynamic textiles that can change their thermal behavior in response to external stimuli. More specifically, shape memory alloys and shape memory polymer coatings have been used for thermal comfort applications. However, the use of shape memory polymers in the form of filament yarns integrated in the fabrics has not yet been reported. These fabrics have some advantages related to versatility in shape design. The aim of this study was to develop woven SMPU-based fabrics with reversible thermodynamic properties induced by weft SMPU filament yarns interlaced into polyester (PES) fabrics. To this end, PES woven fabrics with different ratios of weft SMPU filament yarns (PES/SMPU 1:0; 3:1; 1:1; 1:3, and 0:1) were developed and their thermodynamic properties (thermal resistance, water vapor resistance, and permeability index), shape memory effect, and mechanical performance were evaluated and compared to the 100% PES reference fabric. All the

¹Eurecat Centre Tecnològic de Catalunya, Unitat de Teixits Funcionals, Mataró, Spain

²Departament de Ciència i Enginyeria de Materials (CEM), Universitat Politècnica de Catalunya (UPC), Terrassa, Spain

³Elisava Barcelona School of Design and Engineering (UVic-UCC), Barcelona, Spain

⁴Textile Engineering Department, Faculty of Technology and Metallurgy, University of Belgrade, Karnegijeva, Belgrade, Serbia

Corresponding author:

Judit Gonzalez Bertran, Departament de Ciència i Enginyeria de Materials (CEM), Universitat Politècnica de Catalunya (UPC), Terrassa 08222, Spain.

Email: judit.gonzalez.bertran@upc.edu



Creative Commons Non Commercial CC BY-NC: This article is distributed under the terms of the Creative Commons Attribution-NonCommercial 4.0 License (<https://creativecommons.org/licenses/by-nc/4.0/>) which permits non-commercial use,

reproduction and distribution of the work without further permission provided the original work is attributed as specified on the SAGE and Open Access pages (<https://us.sagepub.com/en-us/nam/open-access-at-sage>).

SMPU-based fabrics developed were classified as extremely breathable (water vapor resistance $<6 \text{ m}^2 \cdot \text{Pa}/\text{W}$) and thermally comfortable (water vapor permeability index <0.3). The fabrics integrating the SMPU filament yarns reacted dynamically to the temperature stimuli over and below T_g , whereas the 100% PES fabric showed passive thermodynamic behavior. This dynamism led to an improvement in thermal protection against an increase in ambient temperature, reaching values of $13.18 \text{ mK} \cdot \text{m}^2/\text{W}$ in thermal resistance (PES/SMPU 0:1), while also maintaining good moisture management properties, reaching values of $5.19 \text{ m}^2 \cdot \text{Pa}/\text{W}$ in water vapor resistance (PES/SMPU 0:1).

Keywords

SMPU, thermal comfort, water vapor resistance, thermal resistance, permanent shape, temporary shape

Introduction

Dynamic reversible textile materials (thermodynamic textiles) are a new generation of textiles that can detect, react, and adapt to external conditions or stimuli such as temperature. To produce these textiles, conventional fibers or yarns are combined with materials like shape memory alloys (SMAs) or shape memory polymers (SMPs) to form woven, knitted, or nonwoven fabrics with dynamic properties.^{1–7} In SMAs, the shape memory effect is produced by the transformation of austenite to martensite and this is applied to textiles in different formats such as filaments or springs.⁸ SMPs are based on the incompatibility of the hard and soft segments in polymer chains, which allows a deformed or temporary shape (TS) to be fixed and returned to the original or permanent shape (PS).⁹ SMPs offer greater versatility in production, a wide variety of shapes, and a high temperature range, unlike SMAs.¹⁰ The relatively low melting temperature of SMPs and their thermoplastic characteristics allow for their production as thin filament yarns, as well as all types of textile finishes (foams, films, and in solution).^{7,11–13} Unlike textile finishes, SMP filament yarns offer higher shape recovery and recovery stress due to the molecular orientation produced by the extrusion process.¹⁴ The shape memory effect (SME) in the form of a filament yarn, once incorporated into the fabrics, is based on its change in length. This change can lead to different effects on the fabrics such as shrinkage, bending and stretching, or increased thickness, among others, depending on the fabric structure.¹⁴ The most suitable SMP for the production of filaments for textile applications is shape memory polyurethanes (SMPUs), due to their adequate mechanical and thermal properties.

One application of shape memory materials is in the production of thermodynamics fabrics for their use in protection and comfort thanks to their temperature-based activation response. These fabrics can change their shape while they adapt to changing environmental conditions, fulfilling the needs of the users.⁸ These textiles allow for an adjustment of the moisture management and warmth characteristics by altering the permeability of the textiles to create a thermal protective barrier against exposure to external heat, improving

the protection performance of the textiles,¹⁵ or with the purpose of creating thermal comfort.¹⁶

Studies that have focused on thermal protection have used SMAs to generate multi-layer active fabrics for protection against low or high temperatures. Bartkowiak et al.⁸ developed a dynamic textile with SMA spring elements programmed to create an air chamber by increasing its height when exposed to a thermal stimulus and shrinking it when the stimulus disappears. The results confirmed that the clothing designed offered a high degree of protection even in extreme thermal conditions. Lah et al.¹⁷ proposed inserting a layer of programmed SMA filament knitted fabric into the traditional protection textile system which, at 75°C, produces bulges that cause sufficient air space to create effective thermal protection. More recently, Wang et al.¹⁸ proposed an improvement of this textile system by reducing the number of layers to four (instead of the five in the traditional system), and integrating the SMA filaments per weft, in an aramid fabric. The thermal protection system was characterized by a normal state of the textile (or temporary shape), with a low resistance to water vapor and temperature, and an activated state of the fabric (or permanent shape) in a hotter environment. The results showed that the SMA system increased thermal resistance and reduced the water evaporation resistance of the fabrics compared to the protective textile system proposed by Lah et al.

Studies focusing on thermal comfort mainly research the use of SMPUs in the form of solution coatings or membranes. One example is Mitsubishi's Diaplex® membrane; a laminate that integrates the membrane between two fabrics. This system allows for the moisture and heat control of the textiles when exposed to a thermal variation, due to the change in the laminate's shape at the molecular level.¹⁹ Another example is the Dermizax® membrane. In this system, when the temperature rises, it produces an expansion of the membrane, increasing permeability and, when it decreases, the pores of the membrane close, keeping the user warm.²⁰ In another study, Memiş and Kaplan²¹ finished wool fabrics with SMPU at different concentrations between 5 and 20 wt.% to evaluate the thermal transfer at temperatures in the range of 20 to 65°C and different relative moisture. The fabric with the best thermal transfer behavior was that with 10 wt.% of SMPU. In a more recent study, an SMPU nanocomposite finish incorporating cellulose nanowhiskers CNWs (SMPU-CNWs) was created to be applied to a polyester knitted fabric for its use in sportswear. The results showed an improvement in the shape memory performance of the knitted fabric, responding to an increase in humidity and temperature by changing permeability, particularly with a 20% CNW content.²² Wang et al.²³ indicated that by optimizing the materials and structure of textiles, it is possible to achieve both thermal protection and moisture management.

The objective of this study was to develop a woven PES plain-weave fabric containing weft SMPU filament yarns with improved thermodynamic properties (thermal resistance and water vapor resistance) and permeability index. According to our knowledge, the use of SMP filament yarns to design a reversible dynamic textile with improved comfort properties has not yet been explored.

For this purpose, SMPU-based fabrics with 100% of PES in warp and SMPU filament yarns interlaced with PES yarns at different ratios (3PES:1SMPU, 1PES:1SMPU, 1PES:3SMPU, 1SMPU meaning 100% of SMPU and 1PES meaning 100% of PES) in weft were

developed. The effect of the SMPU filament content on the thermodynamic properties (thermal resistance and water vapor resistance), water vapor permeability index, shape memory behavior (the shape fixity and recovery ratios), and mechanical properties (tensile tests) was analyzed.

Materials and experimental methods

Materials

SMPU filament yarns with a glass transition temperature (T_g) of 45°C were used. This filament was produced by melt spinning using SMPU (MM4520) pellets provided by SMP Technologies, Japan using a Collin Tech-Line extruder. The details of this melt spinning process have previously been described.²⁴ For the weaving process, the SMPU filament yarns were used in the temporary shape (TS) produced during the extrusion process by passing the extruded filament through an oven (at 80°C). This oven was located between two stretching roller zones with different speeds (15 m/min for the first zone and 32 m/min for the second).

Figure 1 shows a diagram of the scheme with the filaments in different forms. On the top, the filament in the extrusion process, in the middle, the filament in the temporary shape after releasing from the tension of the drawing rollers, and finally, at the bottom, the filament in permanent shape, after heating the sample above T_g (45°C) to a minimum reference temperature of 80°C . This T_r is the temperature required to erase the memory shape from the temporary shape,²⁵ and was determined in a previous study.²⁴

The main characteristics of the SMPU filament yarns used are presented in Table 1.

The recovery length in the permanent shape (PS) was obtained by heating the SMPU filament yarns above the T_g without the application of any external stress. This process

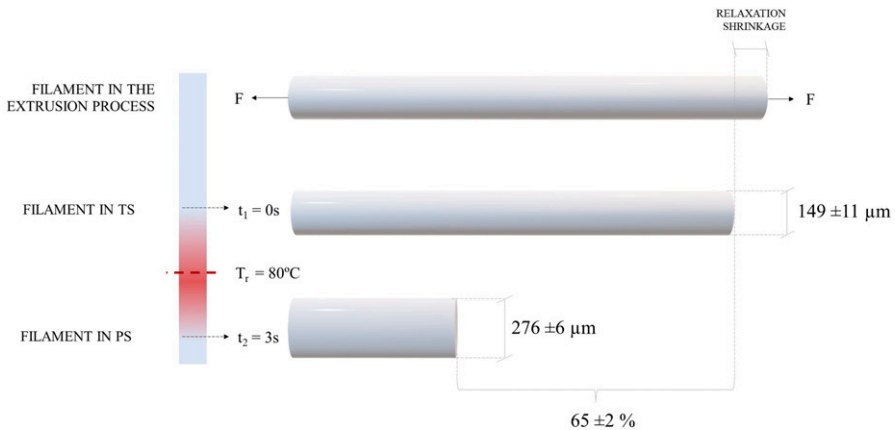


Figure 1. Scheme of the contraction by relaxation after the extrusion process, the diameter of the filament in temporary and permanent shape (TS and PS), the minimum reference temperature (T_r) and the time (t) to return to the permanent shape of the used SMPU filament yarn in this study.

Table 1. Diameter and linear density in the temporary shape (TS) and permanent shape (PS), and percentage of length recovery in the permanent shape (PS) of the SMPU filament yarn used in this study.

Nomenclature	Diameter TS (μm)	Linear density TS (dtex)	Diameter PS (μm)	Linear density PS (dtex)	Length recovery PS (%)
SMPU filament yarn	149 ± 11	253	276 ± 6	748	65 ± 2

allowed for the recovery of the permanent shape by releasing the internal stress of the SMPU filament yarns generated during the extrusion process when producing the temporary shape.

Twisted PES yarns of 450 dtex and 300 dtex, which were kindly supplied by Antex (Spain), were used for the warp (450 dtex) and the weft (300 dtex), respectively.

Experimental methods

Plain weave fabrics were produced using a 45 cm-width laboratory loom (Studio 5020, Techn inc, Taiwan). The warp tension and the rapier speed were adjusted to allow for the correct introduction of SMPU filament yarns per weft. As previously mentioned, SMPU filament yarns were incorporated into the temporary shape (see characteristics in Table 1). The same warp and weft density was used for all the fabrics (22 y/cm and 19.5 p/cm, respectively). PES yarns were used in both warp and weft directions and SMPU filaments were introduced exclusively per weft at different ratios: 3PES:1SMPU, 1PES:1SMPU, and 1PES:3SMPU. For comparative purposes, 100% PES plain-weave fabric (1PES) and plain-weave fabric with 100% SMPU filament yarn per weft (1SMPU) were also produced (see Figure 2). The weft ratio and sample nomenclature used for the different SMPU-based fabrics developed are summarized in Table 2.

To recover the permanent shape after the weaving process, the textiles were heated up to the minimum reference temperature of 80°C. This process was performed without applying any external force using a STUART Digital Hotplate SD 500. Figure 3 shows a simplified scheme of the switching between the temporary shape (Figure 3, left) and the permanent shape (Figure 3, right) due to an increase in temperature over the T_g .

Characterization techniques

For the basic characterization, the warp and weft density were determined using a thread counter, and the areal weight and thickness according to ASTM D3776 and UNE 40,339:2002, respectively. The referred values were the average of at least three measures. The dimensional (width) changes of fabrics directly after the weaving process (relaxation shrinkage) and when they were subjected to heating over T_g were also measured and referred to as the TSF (temporary shape of the fabric) and PSF (permanent shape of the fabric). Five measurements were taken along the fabric in the weft direction (TSF and PSF).

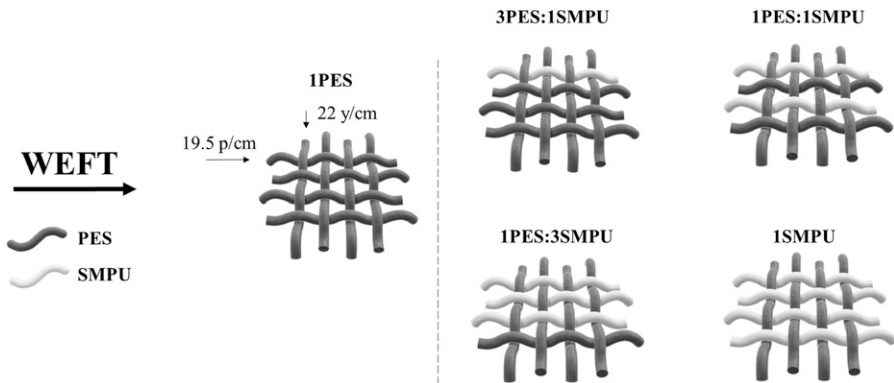


Figure 2. Scheme of the plain-weave fabrics with 100% PES and different PES/SMPU ratios (3PES:1SMPU; 1PES:1SMPU; 1PES:3SMPU, and 1SMPU) per weft (PES in dark and SMPU in light).

Table 2. Sample nomenclature and weft ratio for SMPU-based fabrics.

Sample nomenclature	Weft ratio	
	PES	SMPU
100PES	1	0
25SMPU	3	1
50SMPU	1	1
75SMPU	1	3
100SMPU	0	1

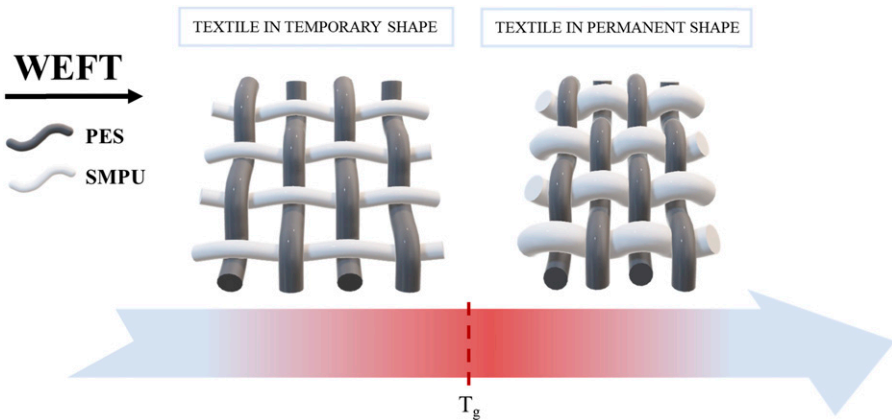


Figure 3. A simplified scheme of the thermodynamics of a plain-weave fabric induced by the presence of weft SMPU filament yarn.

The fabric tightness was calculated using equations (1)–(4).^{26,27} The tightness take into account: the weave factors (K_I), warp and weft density in the TSF, (once the sample was removed from the loom) and in the PSF; and the number of yarns. The maximum density coefficient (K_{dmax}) was determined using the following equations (1) and (2):

$$K_{dmax(weft)} = \frac{Q}{1 + (0.73 \times K_{I(warp)})} \text{ and } K_{dmax(warp)} = \frac{Q}{1 + (0.73 \times K_{I(weft)})} \quad (1)$$

$$K_{dmax} = K_{dmax(weft)} + K_{dmax(warp)} \quad (2)$$

where:

$K_{I(weft)}$ – $K_{I(warp)}$, Galceran weave factors in warp and weft directions.

$K_{dmax(weft)}$ – $K_{dmax(warp)}$, maximum warp-weft density coefficient.

Q , coefficient that depends on the type of matter. In the case of the PES, it is 9.6 and for SMPU (PUR) it is 9.63.

K_{dmax} , maximum warp-weft density coefficient.

The weft-warp density coefficient ($K_{d(tex)}$) was also calculated with equation (3) for each textile with different PES/SMPU ratios:

$$K_{d(tex)} = \frac{D}{\sqrt{N}} \quad (3)$$

where:

$K_{d(tex)}$, warp-weft density coefficient.

D , warp-weft density (y/cm – p/cm).

N , warp-weft yarn linear density (Tex).

Using the previous results, the tightness was determined by means of the equation (4):

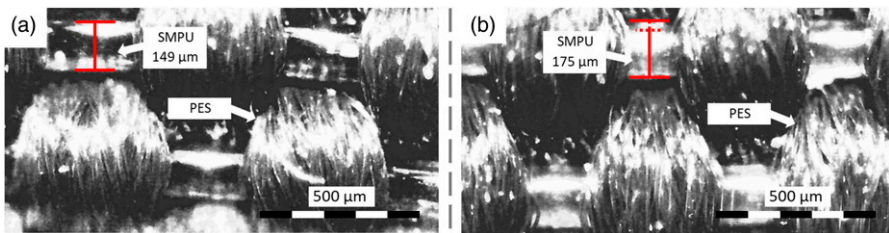


Figure 4. Microscopic image of a 100SMPU textile in the two shapes: (a) TSF and (b) PSF.

$$\% \text{ tightness} = \frac{K_{d(\text{tex})} \times 100}{K_{d\text{max}}} \quad (4)$$

Given that the integrated SMPU filament yarns did not fully recover their permanent shape (that is, their initial diameter and length) after the heat treatment over T_g , to calculate the tightness, it was necessary to determine the diameter of the filament yarns in each of the fabrics produced. Figure 4 shows an example of the microscopic images used to determine the diameters of the filament yarns in the TSF and the PSF.

The water vapor resistance (R_{et}), relative water vapor permeability (RWVP), and thermal resistance (R_{ct}) of the fabrics were determined using a Permetest skin model instrument by Czech Sensor company. Three specimens of 100PES with different PES/SMPU ratios (in both shapes, TSF and PSF) with 150 mm × 150 mm dimensions were used. All tests were performed at $22 \pm 1^\circ\text{C}$ and $44 \pm 1\%$ RH. The relationship between both parameters, R_{et} and R_{ct} , gives the water vapor permeability index (i_{mt}) and indicates the degree of thermal comfort.^{28–30} This index is calculated in accordance with the standard ISO 11,092 using equation (5):

$$i_{mt} = S \frac{R_{ct}}{R_{et}} \quad (5)$$

where the S factor has a value of 60 Pa/K and is used to normalize the units of measure. i_{mt} is dimensionless and has values between 0 and 1. When i_{mt} equals 0 (waterproof fabric) and 1 (permeable fabric).³¹

The mechanical properties were characterized through tensile test, conducted in the weft direction according to UNE-EN ISO 13,934–1: 2013 standard using a static testing Zwick/Roell machine. Five specimens in the PSF of 50 mm width and 100 mm length in the weft direction were prepared for each fabric. A preload force of 5N was applied and the testing speed was set to 100 mm/min.

To determine the shape memory effect (SME), the temporary shape fixation (fixity ratio, R_f), and the recovery to permanent shape (recovery ratio, R_r) different tests were performed using a Zwick/Roell dynamometer test machine. Two types of tests were carried out: one applying a limit recovery force of textile memory (F_1) of 25N at 80°C (T_r) and the other applying the same force at room temperature according to previous studies.^{25,32} The tests were carried out in the weft direction and the values were obtained from the average of three tests. The dimensions of the specimens were 50 × 100 mm.

For the first test, the fabrics were heated up to T_r (80°C) at a heating rate of $5^\circ\text{C}/\text{min}$. Then, T_r was maintained for 1 min and a constant deformation of 10 mm/min was subsequently applied until F_1 (25N) was reached. Afterward, the F_1 was maintained while the sample was cooled down to $21^\circ\text{C} \pm 0.5$ (taking into account the potential application of the textiles developed), keeping it at this temperature for 10 min, until reaching the maximum deformation (ϵ_m). Upon removing the force, there was a small recovery of the deformation (ϵ_u). Finally, the fabric was heated again up to T_r at $5^\circ\text{C}/\text{min}$ to recover the permanent shape, where a permanent residual strain (ϵ_p) was produced. The following formulas were used to calculate the ratio of fixity (6) and recovery (7)^{33,34}:

Table 3. Fabric structure parameters: warp density, thickness, and weight in the TSF and PSF.

Sample nomenclature	Warp density (y/cm)	Thickness at 0.5 kPa (μm)	Areal weight (g/m^2)	Tightness (%)
TSF				
100PES	22.5 \pm 0.0	369 \pm 7	184 \pm 0	74.2 \pm 0.0
25SMPU	24.1 \pm 0.1	374 \pm 13	188 \pm 0	77.1 \pm 0.1
50SMPU	25.0 \pm 0.3	451 \pm 14	197 \pm 0	78.8 \pm 0.7
75SMPU	25.0 \pm 0.3	515 \pm 10	202 \pm 0	78.5 \pm 0.6
100SMPU	25.0 \pm 0.4	524 \pm 13	210 \pm 0	78.8 \pm 0.7
PSF				
100PES	22.7 \pm 0.0	372 \pm 8	187 \pm 0	75.3 \pm 0.0
25SMPU	25.3 \pm 0.2	420 \pm 7	194 \pm 0	80.2 \pm 0.4
50SMPU	28.3 \pm 0.4	462 \pm 22	213 \pm 1	86.8 \pm 0.8
75SMPU	29.3 \pm 0.2	631 \pm 12	233 \pm 0	89.4 \pm 0.5
100SMPU	29.9 \pm 0.5	754 \pm 30	255 \pm 1	91.6 \pm 1.0

$$R_f(\%) = \frac{\varepsilon_u}{\varepsilon_m} \times 100 \quad (6)$$

$$R_r(\%) = \frac{\varepsilon_m - \varepsilon_p}{\varepsilon_m} \times 100 \quad (7)$$

For the second test, a constant deformation of 10 mm/min at room temperature (21°C) was applied until F_1 was reached. Then, the test followed the same steps as the first test.

All the results obtained were statistically treated by means of an analysis of variance (ANOVA) with a Tukey's test being performed using a Minitab software, which provided the significance groups.

Results and discussion

The thermodynamics of the fabric developed is based on the deformation of a woven fabric (temporary shape) to create a more open structure and return the fabric to a more closed structure (permanent shape), leading to the dynamic changes in the length and the diameter of the SMPU filament yarns by an external thermal stimulus. These length and diameter changes affect the fabric structure parameters. Table 3 shows the values of warp density, thickness, areal weight, and the tightness of the fabrics where weft SMPU filament yarns are in both temporary (TSF) and permanent shape (PSF).

As expected, the warp density, thickness, areal weight, and tightness of the fabrics in the TSF are higher for the SMPU fabrics with respect to the 100PES sample. This increase is due to the higher elastic recovery of the weft SMPU filament yarns after the weaving process with respect to the 100PES fabric where no SMPU filament yarns were present. However, regardless of the content of SMPU filament yarns in the TSF, no significant differences in terms of warp density, and fabric tightness were found.

Table 4. Weft shrinkage in the temporary shape TSF (after weaving), weft shrinkage in permanent shape PSF (after the heating treatment over T_g), and residual weft shrinkage (difference between PSF and TSF).

Sample nomenclature	Weft shrinkage, TSF (%)	Weft shrinkage, PSF (%)	Residual weft shrinkage (PSF-TSF) (%)
100PES	2.2 ± 0.0	2.9 ± 0.0	0.7 ± 0.0
25SMPU	8.9 ± 0.2	13.0 ± 0.6	4.1 ± 0.5
50SMPU	12.1 ± 1.2	22.2 ± 1.1	10.1 ± 0.1
75SMPU	12.0 ± 1.2	24.8 ± 0.6	12.8 ± 0.6
100SMPU	12.6 ± 1.3	26.5 ± 1.3	13.9 ± 0.6

The fabrics in the permanent shape (PSF) presented significantly higher values for warp density, fabric thickness, areal weight and tightness when compared to the ones in the temporary shape (TSF). This may be due to the elastic recovery of the SMPU filament yarns and the decrease in length and increase in diameter after the heat treatment over T_g leading to a return to the permanent shape. Moreover, it is clear that 100% PES has almost the same values as all the parameters presented in Table 3 regardless of heating treatment i.e., switching between TSF and PSF, demonstrating no thermodynamic properties (passive textile). This increase was more significant for fabrics with a higher content of SMPU filament yarns, leading to a notable increase in terms of thickness. It was found that the differences in density, thickness, and weight of all the fabrics with SMPU compared to the 100PES were significant according to the Tukey's test.

Table 4 shows the weft dimensional change (weft shrinkage) of the fabric after the weaving process (in the TSF) and after the heat treatment over T_g (in the PSF), calculated regarding the weft length during the weaving process. It also shows the difference between the weft shrinkage in the PSF and the TSF referred to as residual weft shrinkage due to the heat treatment.

As expected, the textiles with SMPU filament yarns presented higher weft shrinkage than the 100PES sample in both the TSF and the PSF. These differences were significant according to the Tukey's test. However, the increase in weft shrinkage is more significant in the case of the PSF due to the effect of heat treatment over the T_g on the SMPU filament yarn/fabrics characteristics, as can be indirectly seen in Table 3. Due to the significant elastic strain recovery (or recoverable deformation) of the SMPU filament yarns over the T_g , the residual weft shrinkage is ruled by their content. The higher the SMPU filaments yarn content, the higher the residual weft shrinkage obtained. However, the residual weft shrinkage was less than expected (maximum of 13.9% in the 100SMPU sample) taking into account that the shape recovery in the length of the SMPU filament yarns that is not integrated into the woven fabric is about 65% (see Table 1). This is due to the high interlacing of the plain-weave fabric's structure, which restricts the full elastic strain recovery of the integrated SMPU filament yarns. This property is of extreme significance for the research objective since achieving a higher elastic strain recovery would imply an improve in thermal insulation (the reduction of heat transfer). Figure 5 shows the fabrics woven for this study in the PS.

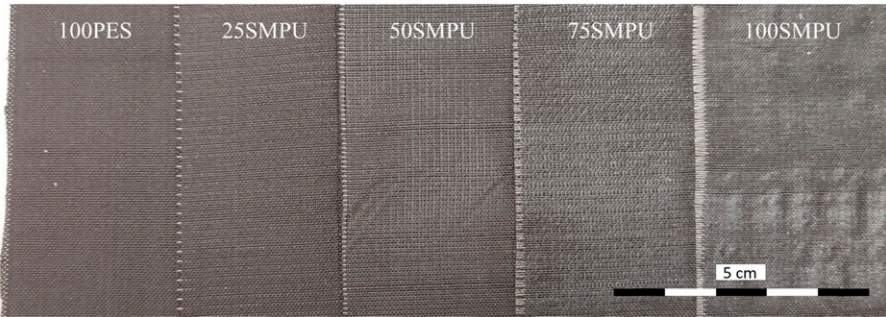


Figure 5. Image of fabrics from this study in PSF.

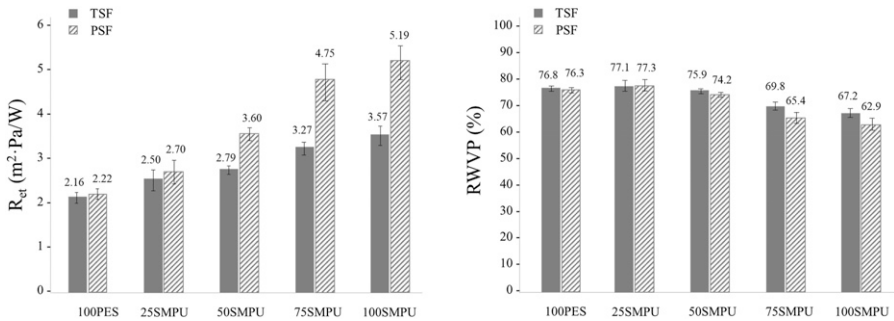


Figure 6. Water vapor resistance (R_{et}) (left) and relative water vapor permeability (RWVP) (right) of the fabrics with different content of SPMU filament yarns (100PES sample used as a reference).

Figure 6 shows the values obtained for the water vapor resistance (R_{et}) and the relative water vapor permeability (RWVP). As shown, the water vapor resistance increases with the SPMU filament content and is higher for the fabrics in the PSF (Figure 6(left)). The differences in terms of water vapor resistance are mainly due to the differences in the thickness and tightness of the fabrics (see Table 3).³⁵ As previously described, incorporating SPMU filaments leads to an increase in thickness and tightness. This increase is more significant for the fabrics in the PSF since the heat treatment over T_g to achieve the permanent state causes the tightening of the plain-weave fabric structure (Table 3 and Table 4). According to the Tukey’s test, the textiles with the highest content of SPMU filament yarns demonstrated significantly higher values of water vapor resistance than the ones in the 100PES sample.

Concerning the RWVP, as shown in Figure 6 (right), increasing the content of the SPMU filament yarns resulted in a significant decrease in the values of the RWVP. This is in a good agreement with the values obtained for R_{et} and confirms better thermal comfort due to the presence of SPMU filaments yarns in fabrics. Although increasing the content of SPMU filament yarns in the fabrics, especially in the PSF form, led to a reduction of the

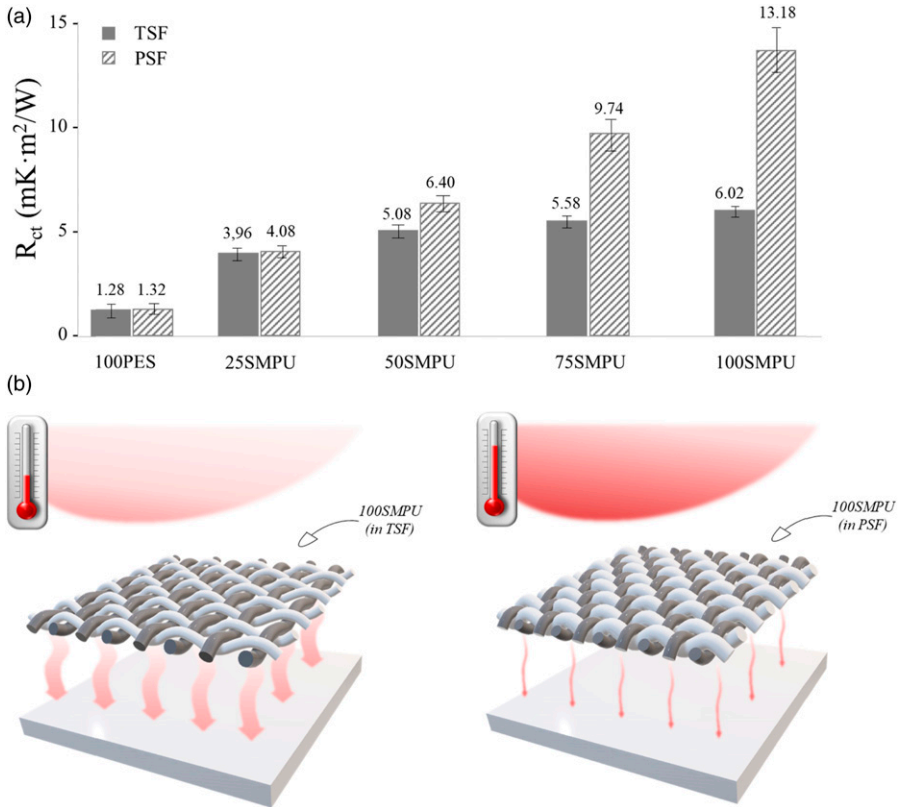


Figure 7. Thermal resistance (R_{ct}): (a) graph for the 100PES sample and the fabrics with SMPU filament yarns and (b) a scheme of the thermodynamic behavior of the SMPU fabrics.

vapor permeability, all SMPU-based fabrics had water vapor resistance values below $6 \text{ m}^2 \text{ Pa/W}$. This indicates that the fabrics are extremely breathable, according to the studies of the comfort rating system by the Hohenstein Institute.³⁰

Similarly, as can be seen in Figure 7(a), the values of thermal resistance R_{ct} increase with the increase in SMPU filament yarn content and are much higher than those for the 100PES fabric. Nevertheless, this increase is more significant for the PSF compared to the TSF, especially for the fabrics with higher content on SMPU filament yarns, demonstrating their thermal sensitivity and reverse dynamic behavior. The differences were significant between the samples with SMPU filament yarns and the 100PES according to the Tukey's test.

The increase in the thermal resistance by the effect of the SMPU filament yarns can be mainly related to the differences in the thickness and tightness of the fabrics, among other parameters.³⁶ In this sense, the fabrics with a higher content of SMPU filament yarns can exert higher thermodynamic comfort against thermal exposition. Figure 7(b) shows this reverse dynamic behavior: the fabric allows thermal protection and moisture management

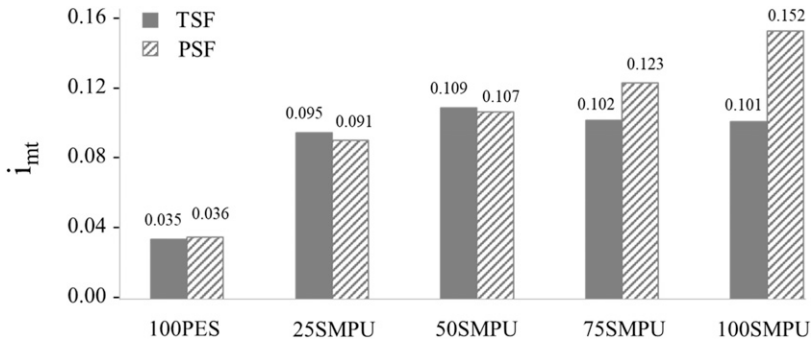


Figure 8. Water vapor permeability index (i_{mt}) of SMPU-based fabric in the TSF and the PSF.

of SMPU at warm temperatures below T_g (Figure 7(b)-left). When temperatures rise over T_g , the thickness and areal weight increase (the fabric is transformed into a permanent shape), regulating the thermal protection on the outside (Figure 7(b)-right). The results of R_{ct} and R_{cl} confirm again that the PES fabric is passive to external temperature stimulus (the values in both the TSF and the PSF are the same).

Figure 8 shows the water vapor permeability index (i_{mt}), calculated from the water vapor resistance and the thermal resistance. The i_{mt} was higher in the fabrics with SMPU filament yarns than in the 100PES fabric. The difference between textiles with SMPU filament yarns in the PSF and the 100PES sample was significant according to the Tukey's test.

All the textiles in the TSF showed similar values, while in the PSF the values increased until reaching 0.15 (100SMPU). This is probably because the increase in tightness and diameter in the PSF has a greater impact on the R_{cl} than on the R_{ct} . According to Verdu et al.,³¹ textiles with vapor permeability index values below 0.3 can be considered thermally comfortable enough to be used as garments. As such, it should be noted that all the textiles developed in this research meet this characteristic, including the 100PES.

Figure 9 shows the relative value increase of each of the thermal parameters analyzed (R_{ct} , R_{cl} , and i_{mt}) for the fabrics with different SMPU content with respect to the 100PES sample.

As shown in Figure 9(a), for the fabrics in the temporary shape, there is a significant increase of R_{cl} and a slight increase of R_{ct} by the effect of SMPU filament yarns with respect to the 100PES sample. This results in an increase in i_{mt} with regard to 100PES while reaching similar values regardless of the SMPU content. However, for the fabrics in the permanent shape (Figure 9(b)), the increase in R_{cl} is clearly higher and R_{ct} is slightly higher compared to fabrics in the temporary shape, thus implying a slight increase in i_{mt} , as seen in Figure 8. This comparison shows that it is possible to improve thermodynamic comfort, given an increase in temperature, with a low impact on the water vapor permeability index, maintaining the fabrics in the thermally comfortable category.

Once it was verified that it was possible to obtain fabrics with reversible thermodynamic comfort by introducing weft SMPU filament yarns, it was analyzed how the

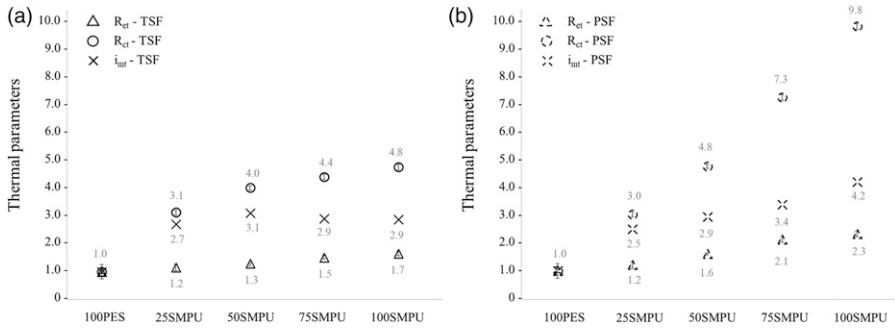


Figure 9. Relative thermal comfort values of the fabrics with SMPU filament yarns with respect to the 100PES sample: (a) fabrics in the TSF and (b) fabrics in the PSF.

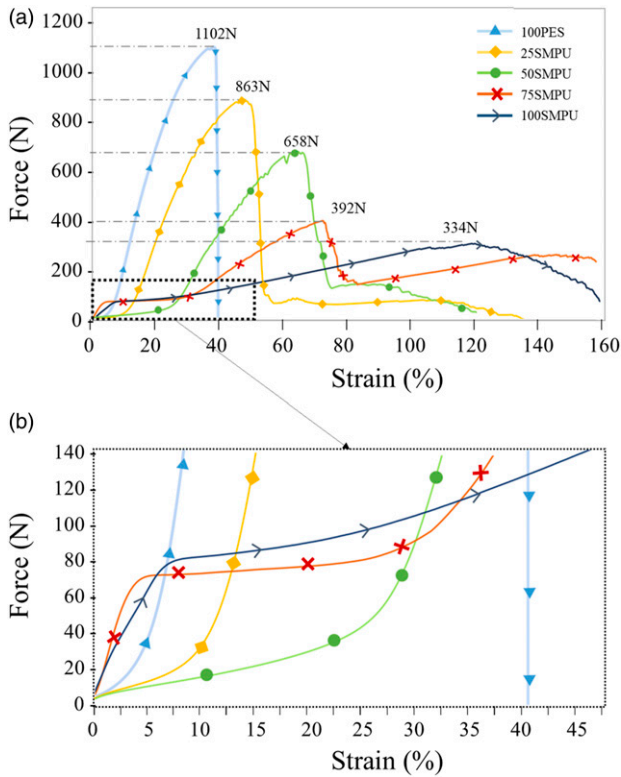


Figure 10. Force-deformation curves obtained from tensile tests of the fabrics with different content of SMPU in the PSF: (a) general graph and (b) detail of the initial zone of the curves up to 50% strain.

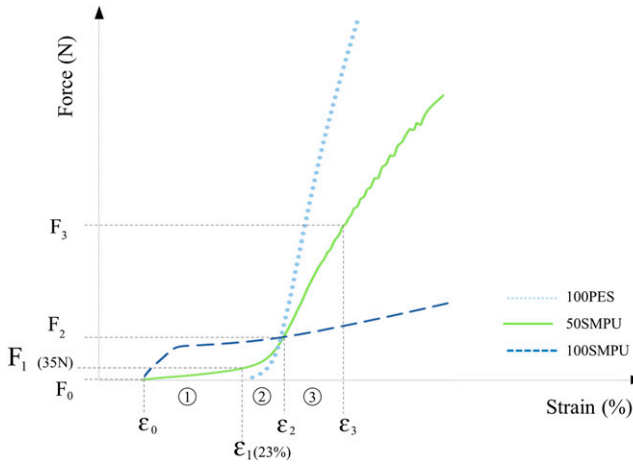


Figure 11. General curves from the force-strain tests performed on textiles with different ratios of PES/SMPU in the PSF.

integration of SMPU filament yarns into the fabrics affects the mechanical performance and the shape memory effect. To this end, the fabrics with different content of SMPU filament yarns were tested in the permanent shape. Figure 10 shows the results of the mechanical properties obtained from the tensile tests performed on the 100PES fabric and the fabrics with different content of SMPU filament yarns. Figure 10(a) shows the full curves obtained until reaching the maximum force at break (F_{\max}) and maximum strain (ϵ_{\max}) and Figure 10(b) shows the detail of the initial zone of the curves.

This graph (Figure 10(a)) shows a superposition of two mechanical behaviors following the superposition model developed by Bruniaux et al.³⁷ and Xiong et al.³⁸ The results of the application of the superposition model on the 100PES (dotted curve), 50SMPU curve (solid green curve), and 100SMPU fabrics (dashed curve) in the PSF are presented in Figure 11. The curve for the 50SMPU fabric demonstrates two main zones, a first zone, between ϵ_0 and ϵ_1 , where the deformation is produced mainly by the SMPU filament yarn, similar to the curve for the fabric with 100% SMPU per weft, showing a low tensile strength and high deformation. The second zone, between ϵ_1 and ϵ_2 , shows a clear increase in tension, produced mainly by the PES fiber, which shows similarities with the curve for the 100% PES fabric, although the increase in deformation indicates that the influence is a result of the combination of both effects, i.e., the 100% PES fabric and the fabric with 100% of SMPU per weft (100SMPU fabric).

This superposition model is applicable to all the curves obtained for the fabrics with SMPU filament yarns, showing a common point that represents the end of the main influence of the SMPU filament yarns and the beginning of the influence of the PES fiber (zone 1). This connection point corresponds to a certain force strain that, in this study, is called limit recovery force (F_1) and limit recovery strain (ϵ_1), respectively.

Table 5. Maximum force (F_{\max}), maximum strain (ε_{\max}) as well as the limit recovery force and strain (F_1 and ε_1 , respectively) obtained for fabrics in the PSF.

Sample nomenclature	F_{\max} (N)	ε_{\max} (%)	F_1 (N)	ε_1 (%)
100PES	1102 ± 18	38 ± 2	22 ± 0	4 ± 0
25SMPU	863 ± 27	48 ± 2	25 ± 1	9 ± 0
50SMPU	658 ± 16	69 ± 3	35 ± 1	23 ± 1
75SMPU	392 ± 4	73 ± 1	87 ± 1	28 ± 1
100SMPU	334 ± 7	128 ± 11	113 ± 1	31 ± 2

In the force-strain graph of [Figure 10\(a\)](#), a decrease in F_{\max} and an increase in ε_{\max} can be observed as the ratio of SMPU filament yarns in the fabrics increased as also presented in [Table 5](#). This characteristic behavior can be attributed to the elastic properties of the SMPU filament yarn. The differences in the values reached in F_{\max} and ε_{\max} of fabrics with SMPU filament yarns compared to 100PES were significant according to the Tukey's test.

[Figure 10\(b\)](#) shows the initial zone in the force-strain curve where the superposition model was applied to obtain the F_1 and ε_1 connection point of the textile models. The parameters calculated from these curves are shown in [Table 5](#).

[Table 5](#) clearly demonstrated that both parameters, F_1 and ε_1 , increased with increasing the ratio of SMPU filament yarns. This increase in F_1 was clearly greater in the 75SMPU and 100SMPU samples than those obtained for 50SMPU and 25SMPU. This phenomenon may be due to the higher concentration of SMPU filament yarns in 75SMPU and 100SMPU, although it will be necessary to carry out more in-depth studies to clarify this phenomenon. The differences in the F_1 of the 75SMPU and 100SMPU samples and in the ε_1 were significant between the samples with SMPU filament yarns and the 100PES according to the Tukey's test.

[Table 6](#) shows the results of the shape memory effect (SME) tests that are determined by the fixity ratio (R_f) and recovery ratio (R_r). As explained in the experimental part, at the beginning of the first test, a minimum reference temperature (T_r) of 80°C was applied and the second test was carried out at room temperature. A limit recovery force (F_1) of 25N, obtained in the force-deformation test, was applied to both ratios. This is the limit force that allows an elastic strain recovery for all fabrics with SMPU filament yarns.

In the test with the initial T_r , the textiles with SMPU filament yarns show high values in the fixity ratio (R_f) and recovery ratio (R_r), which increase with an increasing amount of SMPU filament yarns, while the 100PES sample shows lower values, especially in the R_f . These differences, in the R_f and R_r , between the fabrics with SMPU filament yarns and the 100PES sample were significant according to the Tukey's test. The values obtained for the fabrics with SMPU filament yarns were similar to those presented by the SMPU filament yarns themselves. The small differences may be due to the influence of the plain weave structure that limits fixity but facilitates the recovery of the integrated filament yarns.

Table 6. Fixity ratio (R_f) and the recovery ratio (R_r) at T_r 80°C and at room temperature.

Sample nomenclature	R_f (%)	R_r (%)
Initial process with T_r 80°C		
100PES	17.0 ± 0.9	84.9 ± 0.4
25SMPU	75.7 ± 2.3	90.7 ± 3.3
50SMPU	76.2 ± 2.5	96.0 ± 1.5
75SMPU	79.7 ± 1.2	97.3 ± 0.6
100SMPU	80.2 ± 0.6	97.9 ± 0.5
Initial process at room temperature		
100PES	18.0 ± 0.5	82.7 ± 2.8
25SMPU	21.6 ± 2.4	99.7 ± 0.2
50SMPU	30.8 ± 2.4	99.6 ± 0.2
75SMPU	51.5 ± 1.6	98.0 ± 1.3
100SMPU	56.9 ± 1.3	98.4 ± 0.6

In the tests carried out at room temperature, a progressive increase in R_f was observed, as the ratio of SMPU filament yarns increased, which did not exceed 57% (100SMPU). The R_r values clearly increased in fabrics with SMPU filament yarns integrated compared to 100PES. These differences in the R_f and R_r results between both tests were due to the temperature used when applying the load since, at room temperature, the internal stresses of the SMPU filament yarns increased. Consequently, when the load was released, part of these stresses were recovered immediately.³⁹

The dynamism regulates heat transmission, generating thermal protection against an increase in the ambient temperature (thermal insulation), and, at the same time, maintaining comfort in moisture management. This behavior depends, to a great extent, on the recovery capacity and shape memory effect of the textiles developed with SMPU filament yarns integrated into their structure.

The results obtained in this study allow for the fabric with the most suitable content of SMPU filament yarns to be chosen depending on the thermodynamic comfort and mechanical properties required by the application. Accordingly, a high percentage of SMPU filament yarns would be mandatory in applications where there is a high thermodynamic comfort. In contrast, a low SMPU filament yarn content would be preferential in applications for high mechanical resistance. The thermodynamic comfort requirements of each application and the availability of a heat source will determine the method used for temporary shape fixity.

Conclusions

In this study, innovative SMPU-based plain-weave fabrics facilitating reversible thermodynamic properties were developed. The use of SMPU filament yarns and their introduction per weft into the plain-weave fabrics with PES matrix in warp resulted in the generation of a smart material with reversible thermodynamic comfort that could be useful for many multi-sector applications.

The results obtained demonstrate a clear dynamism of the SMPU-based fabrics compared to the passive response of the 100% PES fabric to the external temperature stimulus. The integration of SMPU filament yarns into the SMPU-based fabrics does not jeopardize the shape memory effect despite the high number of interlacing between PES/SMPU filament yarns present in the plain-weave structure. However, the interlacing between PES/SMPU filament yarns limits the full elastic strain recovery of the integrated SMPU filament yarns to a level lower than in SMPU alone (before the integration into the SMPU-based fabric).

The mechanical properties of the SMPU-based material decreased when compared with 100% PES fabric and this decrease is dependent on the SMPU filament yarn content. However, the decrease in breaking force is compensated by a significant improvement in the elastic strain recovery of SMPU-based fabric after the heat treatment over T_g . The selection of the proper SMPU filament yarn content for integration into the SMPU-based plain-weave fabric is an application-driven process.

The main advantages of SMPU-based fabrics, compared to other kind of thermo-dynamic fabrics, is that the former offer greater versatility in shape design, being able to manufacture different geometries and sizes, and different activation temperatures. Compared to solutions using shape memory coatings, SMPU-based fabrics have greater durability over time as their functionality is integrated into the structure of the material itself. Another advantage is that the SMPU filament, having a molecular orientation given by its manufacturing process, has a higher recovery stress to the permanent shape, compared to coatings.

Acknowledgements

This work was financially supported by the Catalan Government through the funding grant ACCIÓ-Eurecat (Project PRIV – Confortex). Special thanks also to Francesc Mañosa and Daniel Roig for the experimental work and material characterization.

Declaration of conflicting interests

The author(s) declared no potential conflicts of interest with respect to the research, authorship, and/or publication of this article.

Funding

The author(s) disclosed receipt of the following financial support for the research, authorship, and/or publication of this article: This work was financially supported by the Catalan Government through the funding grant ACCIÓ-Eurecat (Project PRIV – Confortex)

ORCID iD

Judit Gonzalez Bertran  <https://orcid.org/0000-0003-4752-3194>

References

1. Boczkowska A. Intelligent materials for intelligent textiles. *Fibres Text East Eur* 2006; 14: 13–17.
2. Wan T and Stylios GK. Shape memory training for smart fabrics. *Transactions of the Institute of Measurement and Control* 2007; 29: 321–336.
3. Hu J, Meng Q and Kong H. Functional shape memory textiles. In: *Functional textiles for improved performance, protection and health*. Sawston: Woodhead Publishing, 2011, pp. 131–162.
4. Gök MO, Bilir MZ and Gürcüm BH. Shape-memory applications in textile design. *Procedia - Social and Behavioral Sciences* 2015; 195: 2160–2169.
5. Tao X. *Handbook of smart textiles*. Germany: Springer Singapore, 2015.
6. Sáenz-Pérez M, Bashir T, Laza JM, et al. Novel shape-memory polyurethane fibers for textile applications. *Text Res J* 2018; 89: 1027–1037.
7. Memiş NK and Kaplan S. Şekil hafızalı polimerler ve tekstil uygulamaları. *Tekstil Ve Muhendis* 2018; 25: 264–283.
8. Bartkowiak G, Dąbrowska A and Greszta A. Development of smart textile materials with shape memory alloys for application in protective clothing. *Materials (Basel)* 2020; 13: 689–717.
9. Wan T. Shape memory polymer yarns. In: *Technical textile yarns*. Sawston: Woodhead Publishing, 2010, pp. 429–451.
10. Sun L, Huang WM, Ding Z, et al. Stimulus-responsive shape memory materials: a review. *Mater Des* 2012; 33: 577–640.
11. Purwar R and Sachan R. Thermoresponsive shape memory polymers for smart textiles. *Advances in functional and protective textiles*. Woodhead Publishing, 2020, pp. 37–62.
12. Zhang F, Xia Y, Liu Y, et al. Nano/microstructures of shape memory polymers: from materials to applications. *Nanoscale Horiz* 2020; 5: 1155–1173.
13. Thakur S and Hu J. Polyurethane: A shape memory polymer (SMP). In: Yilmaz F. (ed) *Aspects of polyurethanes*. Intechopen, 2017, pp. 53–71.
14. Hu J, Meng H, Li G, et al. A review of stimuli-responsive polymers for smart textile applications. *Smart Mater Struct* 2012; 21: 053001.
15. Ma N, Lu Y, He J, et al. Application of shape memory materials in protective clothing: a review. *The Journal of The Textile Institute* 2019; 110: 950–958.
16. Tabor J, Chatterjee K and Ghosh TK. Smart textile-based personal thermal comfort systems: current status and potential solutions. *Adv Mater Technol* 2020; 5: 1901155–1901240.
17. Šalej Lah A, Fajfar P, Kugler G, et al. A NiTi alloy weft knitted fabric for smart firefighting clothing. *Smart Mater Struct* 2019; 28: 065014.
18. Wang L, Pan M, Lu Y, et al. Developing smart fabric systems with shape memory layer for improved thermal protection and thermal comfort. *Mater Des* 2022; 221: 110922.
19. Chakraborty JN, Dhaka PK, Sethi AV, et al. Technology and application of shape memory polymers in textiles. *Res J Text Appar* 2017; 21: 86–100.
20. Gök MO, BİlİR MZ and Gürcüm BH. Shape-memory applications in textile design. *Procedia - Social and Behavioral Sciences* 2015; 195: 2160–2169.
21. Memiş NK and Kaplan S. Wool fabric having thermal comfort management function via shape memory polyurethane finishing. *The Journal of The Textile Institute* 2020; 111: 734–744.

22. Korkmaz Memiş N and Kaplan S. Smart polyester fabric with comfort regulation by temperature and moisture responsive shape memory nanocomposite treatment. *J Ind Text* 2022; 51: 7920S–7941S.
23. Wang Y, Yu X, Liu R, et al. Shape memory active thermal-moisture management textiles. *Composites Part A: Applied Science and Manufacturing* 2022; 160: 107037.
24. Gonzalez J, Ardanuy M, Gonzalez M, et al. Polyurethane shape memory filament yarns: melt spinning, carbon-based reinforcement, and characterization. *Text Res J* 2022; 1: 00405175221114165.
25. Yang Q and Li G. Investigation into stress recovery behavior of shape memory polyurethane fiber. *J Polym Sci Part B: Polym Phys* 2014; 52: 1429–1440.
26. Galceran V. *Influencia de la estructura del hilo y del tejido sobre su rigidez de flexión*. Terrassa: Legal depo, 1961.
27. García Ovejero R. *Estudio del comportamiento de materiales textiles en relación con la electricidad estática*. Diss. Universidad de Salamanca, 2014.
28. Sitvjenkins I, Forces NA, Vilumsone A, et al. Combat individual protection system evaluation of functional replay thermal resistance R_{ct} , water vapour resistance R_{et} and water vapour permeability index i_m . *Sci J Riga Tech Univ Mater Sci Text Cloth Technol* 2011; 6: 81–91.
29. Marolleau A, Salaun F, Dupont D, et al. Influence of textile properties on thermal comfort. *IOP Conf Ser: Mater Sci Eng* 2017; 254: 182007.
30. Reljic M, Stojiljkovic S, Stepanovic J, et al. Study of water vapor resistance of Co/PES fabrics properties during maintenance. In: *Experimental and numerical investigations in materials science and engineering*. Cham: Springer, 2018, pp. 72–83.
31. Verdu P, Rego JM, Nieto J, et al. Comfort analysis of woven cotton/polyester fabrics modified with a new elastic fiber, part 1 preliminary analysis of comfort and mechanical properties. *Text Res J* 2009; 79: 14–23.
32. Juan YH, Wong YC, Wang LJ, et al. Characterization methods for shape-memory polymers. *Chinese J Radiol* 2009; 34: 253–261.
33. Sáenz-Pérez M, Laza JM, García-Barrasa J, et al. Influence of the soft segment nature on the thermomechanical behavior of shape memory polyurethanes. *Polym Eng Sci* 2018; 58: 238–244.
34. Lee SH, Kim JW and Kim BK. Shape memory polyurethanes having crosslinks in soft and hard segments. *Smart Mater Struct* 2004; 13: 1345–1350.
35. Arumugam V, Mishra R, Militky J, et al. Thermal and water vapor transmission through porous warp knitted 3D spacer fabrics for car upholstery applications. *The Journal of The Textile Institute* 2018; 109: 345–357.
36. Nayak R, Kanesalingam S, Houshyar S, et al. Effect of repeated laundering and Dry-cleaning on the thermo-physiological comfort properties of aramid fabrics. *Fibers Polym* 2016; 17: 954–962.
37. Bruniaux P, Crepin D and Lun B. Modeling the mechanics of a medical compression stocking through its components behavior: Part 1 - modeling at the yarn scale. *Text Res J* 2012; 82: 1833–1845.
38. Xiong Y and Tao X. Compression garments for medical therapy and sports. *Polymers (Basel)* 2018; 10: 663–719.
39. Zhu Y, Hu J, Yeung LY, et al. Development of shape memory polyurethane fiber with complete shape recoverability. *Smart Mater Struct* 2006; 15: 1385–1394.